Oscillating-Flow Regenerator Test Rig: Final Report

J. G. Wood

D. R. Gedeon

September 26, 1994

(NASA-CR-196982) OSCILLATING-FLOW REGENERATOR TEST RIG Final Report, 1 Apr. 1991 - 26 Sep. 1994 (Ohio Univ.) 34 p

Final Report Prepared for NASA-Lewis Research Center

Grant Number	NAG3-1269
Grant Title	Measurement of Heat Transfer in Regenerators Under Oscillating Flow Conditions
Principal Investigator:	J. G. Wood
Performing Institution:	Center for Stirling Technology Research, Ohio University
Reporting Period	4/1/91 - 9/26/94

CONTENTS

SUMMARY

This report summarizes work performed at Ohio University's CSTR (Center for Stirling Technology Research) in setting up and performing testing on a regenerator test rig. This work was performed under NASA grant NAG3-1269. An earlier CSTR status report [1] presented test results, together with heat transfer correlations, for four regenerator samples (two woven screen samples and two felt metal samples).

Lessons learned from this testing led to improvements to the experimental setup, mainly instrumentation, as well as to the test procedure. Given funding and time constraints for this project it was decided to complete as much testing as possible while the rig was set up and operational, and to forego final data reduction and analysis until a later date. Additional testing was performed on several of the previously tested samples as well an on five newly fabricated samples. The following report is a summary of the work performed at OU, with many of the final test results included in raw data form.

Those interested in heat transfer results only may wish to skip the sections on rig set up and debugging. These are included mainly to document the work here and justify changes performed on the hardware.

BACKGROUND

The regenerator test rig is a modified form of an earlier pressure drop test rig designed by Sunpower Inc. for NASA-Lewis. This pressure drop test rig was used to perform extensive oscillating flow pressure drop testing on heat exchangers and regenerators typical to those used in Stirling engines.

Details of the original pressure drop test rig can be found in reference [2]. The basic rig is based on a variable stroke and variable frequency linear drive motor. A displacement section, consisting of a single close fitting piston in a cylinder, is directly attached to this linear drive motor. The test section is connected to the other end of the displacement section. The assembled motor, displacement, and test section are then enclosed in an outer pressure vessel to allow for operation at largely elevated mean pressures.

The versatility of the basic test rig is shown by the wide range of operating parameters listed in the following table.

Stroke:	0 -	3.0 cm.	
Frequency:	<1 -	120 Hz.	
Mean Pressure:	0 -	151 bar	(absolute)
Motor Power:		2 kW	(at 60 Hz., 3 cm. stroke)
Piston Diameter:		1.9 cm.	(standard configuration, larger and smaller pistons possible)

REGENERATOR TEST RIG DESIGN

In order to perform regenerator heat transfer testing, the test section of the original pressure drop rig (comprised of a single element test section) was replaced by a multiple element unit consisting of a cooler, regenerator, heater and an insulated buffer volume. The design, fabrication and implementation of this setup was performed by Sunpower Inc. for NASA- Lewis under contract NAS3-25620. A detailed description of this hardware is given in reference [3]. A description of this hardware, together with modifications made at OU, will be given later in the present report.

Before delivery to OU the test rig had been operated only once to check basic operation. However, the rig had not been debugged, nor had the original data acquisition system been expanded to handle the numerous new instrument signals (mostly thermocouples).

The original run had apparently been performed at atmospheric pressure, since the rig was found at OU to be incapable of holding pressure due to numerous leaks. These leaks existed in the pressure vessel extension which was part of the new arrangement.

Another uncompleted task was that of wiring up all the new instrument signals. Provisions had been made for this by means of numerous ports for wire feed throughs in the pressure vessel extension. However the wiring had not been completed.

Because of the condition of the rig as stated above, the task of setting up the rig was much more involved than expected. Significant remaining work was required to make the rig truly operational, as well as in the debugging process. The following sections detail the work performed here.

SETUP OF THE REGENERATOR TEST RIG AT OU

Hydrostatic Testing of the Outer Pressure Vessel
The pressure vessel of the original pressure drop test rig had been hydrostatically tested. However the new layout included an untested pressure vessel extension, through which the numerous new instrument wires crossed the pressure wall.

To insure the new arrangement was safe, the entire pressure vessel was therefore hydrostatically tested to 1.5 times its design pressure. Early in this process many of the pipe thread fittings in the pressure vessel were found to be quite troublesome.

These threads were located near the weld joint between the wall and the flange of the pressure vessel extension. Apparently the area of the threads had been distorted during the welding process. The leakage problem was solved by re-tapping the threads. Following this the vessel was successfully hydrostatically tested.

Expansion of the DAS (Data Acquisition System)
In order to handle the numerous new instrument signals of the regenerator test rig a 32 channel submultiplexer board was obtained and installed.

Because of a limited budget we selected a board, supposedly equivalent to a Metrabyte board, but which was lower in cost. This decision turned out to be much more costly than the money saved in the purchase of the board itself.

Suspicious temperature indications led us to check out the entire data system, suspecting ground loop problems. It was finally determined that the board's open circuit detect resistor was much smaller than that of a Metrabyte board. This resulted in the temperature readings being very sensitive to thermocouple extension wire lengths. The matter of determining this was complicated by the fact that the manual for the submultiplexer board contained an incorrect circuit diagram.

Writing of DAS Software
DAS software was written by Eric Bakeman, a software consultant with experience in test rigs similar to the regenerator test rig.

Installation of Signal Lines Between the Rig and the DAS
Significant time and labor was consumed here in wiring up all the signal lines. This task was complicated by the extremely cramped quarters inside the pressure vessel extension and also by the involved rig assembly/disassembly process.

Redesign of the Heater Section
The heater section was initially designed as a shell and tube heat exchanger. Heat was supplied by means of a pumped Dowtherm closed loop. Here the heating element and the pump were external to the outer pressure vessel, with the fluid carrying lines passing into the vessel through the pressure vessel extension.

Besides the assembly difficulties associated with the fluid lines, this system appeared all too complicated and trouble prone. Problems were anticipated not just in sealing the loop, but also in long times required to reach steady state operation between test runs.

Here we decided to replace the heater with a copper cylinder having drilled flow passages. Heating was supplied be means of two stock band heaters clamped to the outside of this cylinder. Heat input was controlled by use of a commercial temperature controller.

PROBLEMS ENCOUNTERED AND SOLVED (THE DEBUGGING PROCESS)

We consider the above to be representative of the process of completing the rig and the test setup. The following explains other problems observed and corrected in the debugging process.

Installation of Capillary Tube to Vent the Buffer Volume
The buffer volume is attached to the end of the heater opposite the end connected to the test section. This is a sealed and thermally insulated canister for the purpose of containing the hot gas exiting the heater.

As originally intended, gas would enter the buffer during the charging process; entering past the close fit piston seal and proceeding through the cooler, regenerator and heater sections.

This would have been fine, except for the limited range of the pressure transducer in the displacement section. This transducer is an Endevco 8510B which has the back side of the sensing element ported to the interior of the outer pressure vessel The maximum range of this transducer is $\pm$ 1.0 bar.

On initial charging we quickly pegged this transducer. This indicated that the piston clearance seal was very effective. However, it made apparent that charging or discharging the rig would take on the order of more than an hour.

At this point we designed a capillary tube to vent the buffer volume to the interior of the outer pressure vessel. Sized so as to give reasonable charging times, while not affecting the accuracy of the measurements.

Convection Problems

In early testing we noticed that the heat flow to the cooler, when the rig was charged but not being cycled, varied with the charge pressure as well as with the gas which was being used. This indicated that significant convective heat losses were occurring inside the rig.

These could have been measured and accounted for, but would have decreased the accuracy of the test results. Perhaps a larger problem was that long time periods would be required before testing at different pressure levels to allow the losses to stabilize.

Here we initially tried to install baffles and shields inside the rig to reduce the problem. Besides further complicating the already difficult assembly of the rig, these seemed to have only limited effects.

The final solution here was to invert the rig for operation. This was a rather troublesome thought in the beginning, because of the large bulk and mass of the assembled rig. However this eventually greatly eased the assembly/disassembly process.

The principal modification here was to weld a lifting eye to what had previously been the bottom of the outer pressure vessel. Test stand adapters were also fabricated to accommodate the new arrangement. The remaining change which eased the assembly process considerably was to omit the bolts which had originally clamped the motor base plate to the outer pressure vessel. Instead of these, elastomeric spacers were used so that motor plate was clamped in place as the vessel was bolted together.

Prior to these changes the rig had to be completely torn down to get to the test section. With the new arrangement, only one flange had to be unbolted and the main pressure vessel lifted off, to expose the test section.

Pressure Vessel Extension O-ring Problems

Early testing was plagued by problems with pressure vessel extension flange O-ring. This O-ring had to be "blown in" to make it seat. The problem here was that the O-ring groove had been cut too deeply, and there was not adequate room to enlarge the groove for a larger cross section O-ring.

This problem was solved by making an O-ring from the next size up metric (this was originally an inch size) O-ring cord.

Sample Holder Fabrication Difficulties

As originally designed the test samples had Viton holders molded around them. The process here was to vulcanize Viton under elevated heat and pressure around the test samples. After this was completed five fine wire thermocouples were installed on each face of the regenerator. The thermocouple wires were laid in small grooves cut into the faces of the Viton holder and sealed with Viton glue.

This had been done successfully at Sunpower for a high density, fine wire sample. In order to learn the molding process we called upon the technician who had fabricated the first sample at Sunpower. Here we asked the technician to demonstrate the process on a new sample of stacked screens, having larger wire diameter and a lower density.

Repeated attempts here proved unsuccessful. The problem seemed to be with the combination of the specific Viton material and the heat and pressure levels applied. After numerous attempts, the parameters were finally adjusted so that the Viton filled the mold and vulcanized correctly. However penetration of the Viton into the sample was severe and very non-uniform.

Another problem which led us to abandon the Viton holder was experienced after an extended run with the sample supplied with the rig. On disassembly of the rig, the holder was found to have strongly adhered itself to the heater flange. Disassembly required severe prying, which eventually ruined the holder. The diffuser disk staid attached to the heater, damaging the thermocouples

We thus abandoned this process and devised alternative simpler methods of holding the sample. We decided to place the samples in Torlon holders. Torlon was selected because of its good temperature and insulating properties, as well as the availability of a particular grade having expansion characteristics almost identical to material of the samples themselves. Two separate methods were devised here, one each for the two different types of samples which we planned to test.

In the case of a sintered rigid material, first round disks of the sample were cut. Torlon holders were then fabricated for heat shrinking around the sample. Samples were cooled with liquid nitrogen and the Torlon heated in an oven before final assembly.

For stacked screen samples, the screens were first aligned and clamped between centers in a lathe. The outside surface of this stack was then coated with a high temperature (260 ^{0}C, 500 ^{0}F) epoxy, and allowed to cure. Once cured, the outside surface of epoxy was machined round. Then several screens were peeled of each face of the sample to determine the level of penetration of the epoxy. Torlon holders were fabricated for each of these samples. Here instead of a heat shrink process the holders were fabricated with inside diameter O-rings for sealing against the outside of the sample.

To provide for the thermocouples and the diffuser disks we fabricated reusable holders for these, separate from the test sample. These were fabricated from G7 phenolic. Sealing on the face of these next to the heat exchangers was accomplished by means of silicone glue. On the faces adjacent to the test sample, sealing was provided by O-rings with the grooves cut into the face of the Torlon holders.

Actually before the final group of testing, in an attempt to increase the operating temperature slightly, we fabricated and assembled a stainless steel diffuser/thermocouple disk for the hot end. However, we were not able to achieve a good seal on all the thermocouple wires, apparently due to the grooves being oversized. Because of time constraints to finish testing, the phenolic disk was reinstalled on the hot end.

Cooler Blockage

During early runs we also discovered that six of the cooler passages were blocked. We discovered this largely because of the problem we had experienced with the Viton adhering itself to the heater. In that case, part of the Viton had actually extruded into the flow passages and had to be removed. The inspection and clean up of the heater led us to inspect the cooler passages.

Apparently the cooler had not been adequately cleaned after the brazing process, for several of its passages were blocked. Here drills and small wires were used by hand to clean out what was apparently silica which had been packed in the tubes before brazing. We were able to clean out all but one of the passages which was apparently blocked with brazing material.

Change of Method of Measuring Coolant Temperature Rise

It was soon apparent to us that use of type K thermocouples for measuring the temperature rise of the fluid was inadequate. We replaced these with high accuracy (0.1 ^{0}C interchangeable) thermistor probes from Omega. Here we obtained several probes (for spares) and selected the two best matched thermistors from the group.

EARLIER REPORTED TEST RESULTS

Once operational and debugged, the rig was used to generate the test results given in the earlier CSTR status report[1]. This report presented reduced test results for the four following samples:

200 Mesh Stacked Screens 200 mesh (per inch) stainless steel wire screens, wire diameter 53.3 microns (0.0021 in), porosity 0.6328, sample length 11.1 mm

200 Mesh Sintered Screens same screen material as above only sintered, porosity 0.6232, sample length 10.1 mm

1.0 Mil Brunswick Brunswick stainless steel metal felt, round wire, 25.4 micron (0.001 in) diameter, porosity 0.8233, sample length 12.9 mm

0.5 Mil Brunswick Brunswick stainless steel metal felt, round wire, 12.7 micron (0.0005 in) diameter, porosity 0.8405, sample length 14.9 mm

In this set of testing the sintered screens were run first. The testing method was improved after the sintered screen tests to include intermixed zero amplitude test points for the purpose of determining static conduction losses. Prior to this static conduction had been measured only twice for a given run, once before and once after a run.

A problem that led to this modified test procedure was the long time required for both the rig and the water supply to come to steady state temperature conditions. This required several hours of rig operation. Additionally, occasional small changes in water supply pressure would also change operating conditions. The new procedure allowed us to account for fluctuations in supply pressure and also provided us with a record of testing which could be examined to determine when things actually stabilized.

TEST RIG AND TESTING PROCEDURE IMPROVEMENTS

Lessons learned from the above testing led to improvements being made to both the experimental procedure and the test setup.

The earlier status report recommended that more test points be taken, weighted at the extremes of Reynold's numbers. This recommendation was followed in all future testing.

Other improvements included increased resolution in the measurement of heat rejection. The original flow sensor supplied with the rig was grossly oversized (Omega model FTB-101: linear range 1.4-14.0 LPM). When using this sensor, water flow was set at the lower end of its linear range. To improve the measurement of heat rejection, a smaller flow meter (COX model LF6-00) was supplied by NASA.

We also attempted a constant head (stand pipe type) system for supplying the coolant. This did not work with the Cox flow meter because of its still fairly high flow range, its high pressure drop, and the limited ceiling height in the test cell.

To solve the problem of coolant temperature changes over time, a laboratory cooling bath was acquired and installed. Water from the wall supply passed through the bath in coiled copper tubing, before proceeding to the test rig.

RETEST OF SINTERED SCREEN AND IMPROVED ERROR ESTIMATES

The sintered screens were then retested with the improved cooling system. Details of this testing is given in Appendix A, a summary is given in the following.

The analysis of these results led to revised error estimates.
A new variable **k..static..err** was introduced to handle observed fluctuations in static heat conduction. The coolant mass flow error estimate **Mdot..err..coolant** was also increased.

Revised correlations obtained were as follows:

Overall Heat Flux $N_q = a_1 P_{em}^{a2}$

where: $a_1 = 0.513 \pm .030$
$a_2 = 1.260 \pm .010$

Simultaneous N_u and N_k: $N_u = a_1 P_e^{a2}$ $N_k - N_{k0} = a^3 P_e^{a2}$

where $a_1 = 0.844 \pm 0.100$
$a_2 = 0.572 \pm 0.020$
$a_3 = 3.561 \pm 0.48$

Effective Nu: $N_{ue} = a_1 P_e^{a2}$, assuming $N_k - N_{k0} = 0$

where $a_1 = 0.288 \pm 0.016$
$a_2 = 0.740 \pm 0.010$

MORE TEST RIG IMPROVEMENTS

The above testing was followed by further improvements to the test rig. In order to improve the measurement of heat rejection even more, we obtained and installed an Omega model FTB601 (linear range 0.1-2.0 LPM) flow sensor. This flow sensor allowed us to reduce coolant mass flow significantly and also allowed us to install a constant head flow system.

TESTING OF NEW SAMPLES AND RETESTING OF OLD SAMPLES

With the new improved test setup we went back and retested several of the earlier samples. The samples retested were:

2.1 mil 200 mesh Sintered Screen
1.0 mil Brunswick
0.5 mil Brunswick (short sample) *

* As recommended in the earlier report a shorter sample of this previously tested material was fabricated. The length of this sample was 7.43 mm (0.293 inch), measured porosity was 0.831 .

Additionally, five new samples were fabricated and tested for both pressure drop and heat transfer.

80 Mesh Stacked Screen Stainless Steel, wire diameter 93.98 microns (0.0037 in), porosity 0.710, sample length 22.08 mm

100 Mesh Stacked Screen Stainless Steel, wire diameter 55.88 microns (0.0022 in), porosity 0.781, sample length 17.53 mm

2.0 mil Brunswick Inconel metal felt, round wire, 50.8 micron (0.002 in) wire diameter, porosity 0.688, sample length 7.544 mm

1.5 mil Brunswick (Top Sample) Stainless Steel metal felt, round wire, 38.1 micron (0.0015 in) wire diameter, porosity 0.730, sample length 7.67 mm

1.5 mil Brunswick (Middle Sample) Stainless Steel metal felt, round wire, 38.1 micron (0.0015 in) wire diameter, porosity 0.748, sample length 7.49 mm

The two samples of the 1.5 mil Brunswick were cut from the same rather thick piece of felt metal. Samples were cut from both the surface (top sample) and from the central area (middle sample) of the material.

FINAL TEST RESULTS

The results of final testing exist mostly in raw data form, as time and money ran out before all the results were reduced. This data is given in Appendix D on floppy disk. Also found in this appendix is a table describing which runs exist in which files.

We did reduce the pressure drop test results for the 80 mesh 0.0037 inch stacked screens, with complete results given in Appendix C. Because of the nature of this screen it was possible to perform testing out to a much higher Reynolds number (Re $\approx$ 6000) than before.

This indicated that a better fit to the data was achieved by using a modified form of the friction factor equation. The form used here is:

$$f=a_1/Re + a_2 Re^{a3}$$

The parameters determined and the 90% confidence intervals for this form are:

$$a_1 = 118.7 \pm 0.3$$
$$a_2 = 2.655 \pm 0.016$$
$$a_3 = -0.09734 \pm 0.00080$$

Heat transfer test results, with the above improvements to the test setup and procedure, were reduced for the shortened sample of 1/2 mil Brunswick. Results of this are given in Appendix B. Equations for Nq and Nue were found comparable to earlier results. However, the new results indicated a shift in relative importance in Nu and Nk.

RECOMMENDATIONS

The raw data of Appendix D still needs to be analyzed and studied in detail. No doubt much useful information and lessons will result from the study of this data.

On the hardware and instrumentation front, the test rig has evolved into a workable and useful piece of hardware. Major problems and difficulties have been worked out here. At present it is a fairly easy to change samples and perform testing.

Some minor hardware changes could be made to improve things further. First off, to increase the temperature differential, a new hot end diffuser/thermocouple holder could be fabricated from stainless steel and installed.

To reduce the time required to reach steady state and thus expedite future testing several things could be done. The primary component here is the buffer volume. This currently is a fairly thick walled vessel having more much more mass, and resulting thermal mass, than necessary. The simplest change here would be to machine the wall of the part to make it thinner. A preferred change would be to make a new buffer of a material having better insulating qualities, such as phenolic.

Also installation of band heaters and insulation to the outside of the main pressure vessel would allow for preheating of this element and again reduce the time to acquire steady state conditions.

REFERENCES

[1] D. Gedeon and J.G. Wood, *Oscillating-Flow Regenerator Test Rig: Woven Screen and Metal Felt Results*, OU Center for Stirling Tech. Research status report to NASA-Lewis (Grant No. NAG3-1269), July 1992

[2] J.G. Wood, E.L. Miller, D.R. Gedeon and G.E. Koester, *Description of an Oscillating Flow Pressure Drop Test Rig*, NASA Tech. Memo. 100905, Aug. 1988

[3] D.R. Gedeon, G. Koester, and Al Schubert, A Test Rig for Measuring the Thermal Performance of Stirling Cycle Regenerators, SBIR Phase 1 report, Sunpower Inc., NASA contract NAS3-25620, (1989)

APPENDIX A: RESULTS OF SINTERED SCREEN RETESTS

Memo

To: Gary Wood
From: David Gedeon
Subject: Regenerator Test Rig: Sintered Screens Rerun
Date: October 6, 1992

A rerun of the sintered-screen data gives different results than before but with improved confidence bands. Improved resolution begins to show weakness in correlating expressions for N_q and N_{ue} but corroborates expressions for N_u and N_k.

Background

We decided to rerun the previous sintered screen heat-transfer tests (data set nh05-07) because, (1) they suffered from relatively high error bands due to insufficient data points logged, (2) they were logged back in the days when the coolant thermistor signals were troubled by 60 Hz noise and (3) static conduction values were logged by hand at the end of test runs.

The present tests correct all of the above problems. There are more data points logged — 193 compared to 59, weighted more toward the low and high Reynolds number extremes than before. Thermistor signals are properly filtered. And static conduction is software-calculated on the basis of several zero-amplitude data points interspersed in each data set.

The cooling system is also a bit different. The present runs used a NASA-donated flow sensor, more accurate at low flow rates than before. But, after data had been logged we discovered that the NASA-supplied calibration was about 5% high for water, our coolant. Rather than re-run all the tests we simply corrected all Mdot_coolant values in our data files. Corrected mass flow rates appear in all .SCN files and their derivatives. They are also the basis for the remainder of this memo. The reason for the calibration error seems to be due to the use of a non-water calibration fluid at NASA.

Present test are in data files logged from 09-18 through 09-21, ultimately combined into master file nh09-18.drv. Low-end R_{em} is significantly lower than before — about 1.6 compared to 4.8. High-end R_{em} is about the same — 1030 compared to 1100.

Residuals

I spent a good bit of time staring at and interpreting residuals in the present data sets. Initially they were about four times too large (suggesting input error estimates about four times too small) — especially at the high R_{em} end. You too can stare at residuals in the *before* picture of figure 1. By definition, normalized residuals should be distributed around zero with a variance of one. I pursued two different theories as to why this was not the case.

New Input Variable k_static_err

Theory one was that we were not taking into account random fluctuations in cooler heat rejection as observed in our static conduction measurements. Thus I was led to introduce a new variable k_static_err in .SCN data files, which is automatically determined by the data screening program on the basis of the standard deviation of static conduction for the usual set of zero-amplitude data points. This requires nothing new on the part of the rig operator. Data translation program RRHTRANS now incorporates k_static_err in its calculation of overall heat flux error Qt_err.

For logical consistency we should also put k_static_err in .RAW data files. This would give the operator a chance to override its value if need be and also keep the format of .RAW files identical to .SCN files. Thus, we should eventually have Eric Bakeman make yet another modification to his REGENRIG program, namely adding k_static_err to the .RAW file header I/O variable list, described as "standard deviation of many k_static measurements taken over the course of a test run", to appear immediately after k_static. The default value should be 0.

Revised Mdot_err_coolant

Taking account of static conduction improved residuals at the low R_{em} end, but did little at the high end. Thus I was led to theory two: that we were underestimating coolant mass flow rate error. This error enters into the Qt_err calculation in a manner that increases in direct proportion to coolant ΔT, which in our case is in direct proportion to R_{em} because of our practice of logging all data with pretty much the same coolant mass flow rate.

So I arbitrarily increased the coolant flow rate error variable Mdot_err_coolant in our .SCN data files. With a bit of experimentation I determined that a value of 2.0E-4 kg/s (compared to 3.63E-5 kg/s initially) produced reasonable looking residuals at the high R_{em} end.

After the above two corrections to our input error estimates, the residuals plotted for simultaneous N_u and N_k reduction looked like the *after* picture of figure 1. According to the data modeling software these are quite reasonable (probability of being too large only about 0.87 compared to about $1 - 10^{-12}$ initially).

It is worth noting that some of the residual plots of the July 29, 1992 status report could also use some work. In my haste to reduce that data I appear to have let pass some residuals that would make my eyes bug out now. You might want to turn to page 23 of that report. Note the stacked screen residuals (upper left) go from too small to too large with increasing R_{em}, similar to the initial problems with the present data set. Residuals for the sintered screen tests (upper right) are uniformly too large. Residuals for the Brunswick cases are not too bad. If we had gobs of time and money I should probably go back

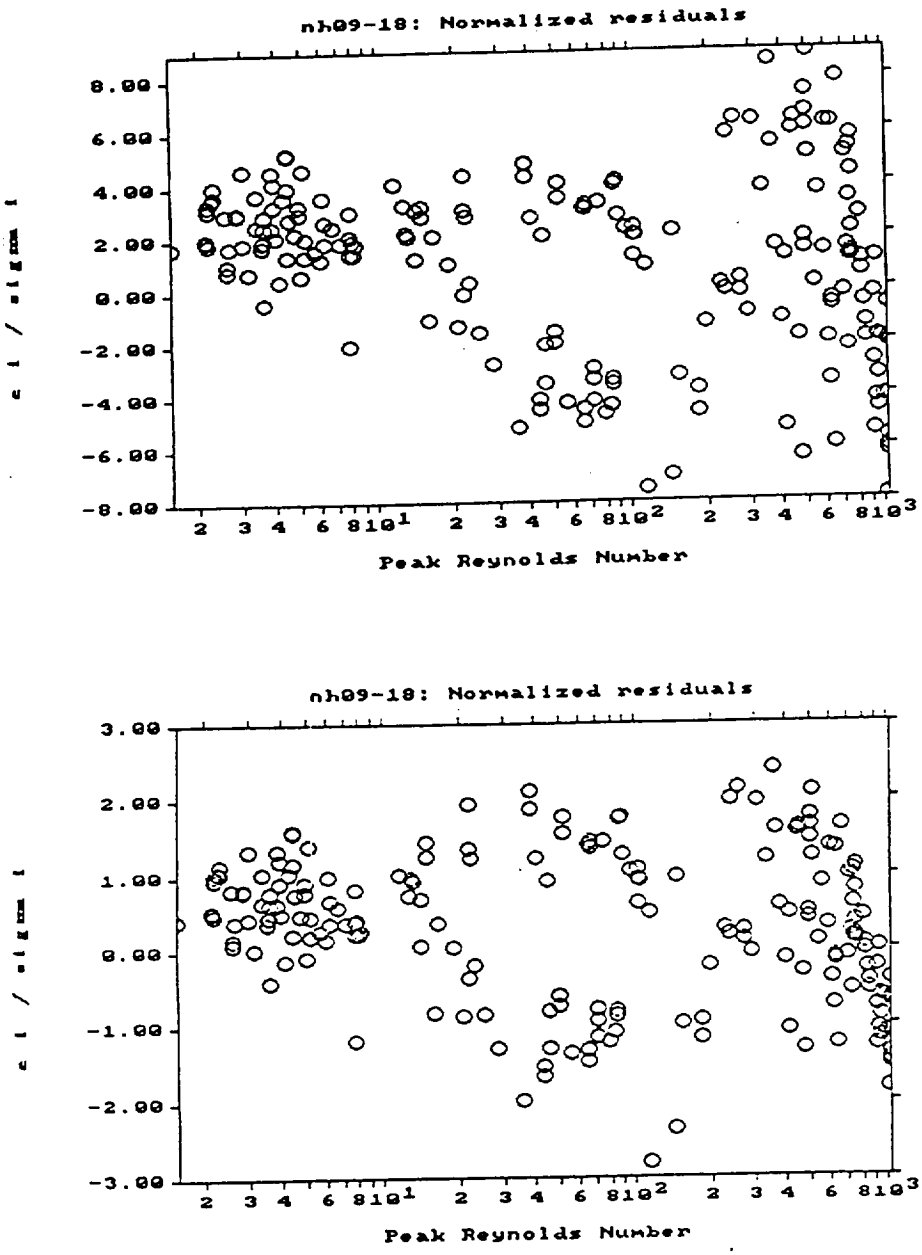

Figure 1: Residuals in the present data set for simultaneous N_u and N_k modeling, before (top) and after (bottom) correcting input error estimates.

and re-reduce at least the stacked screen data. But I am deferring this for later so that I don't run out of time before getting to the meat of the present contract phase.

Bad Confidence Intervals and Skewed Curves

Perhaps you are wondering just why residuals are so important. There are two reasons. First, they affect the confidence intervals printed by the data modeling program. Second they can skew correlating curves to favor the low or high R_{em} range.

Confidence intervals scale in direct proportion to the input estimated errors — at least the way the present software works. If estimated errors are too small then confidence intervals will also be too small (optimistic). Residual plots give us an easy way to check that our estimated errors are valid. From now on we should always make sure our residuals are reasonable before publishing parameter estimates. By the way, confidence intervals are inversely proportional to $\sqrt{N}$ where N is the number of data points logged.

Curve skewing occurs whenever residuals grow systematically toward one end of the R_{em} scale or the other. The reason is simply that the data modeling software will work harder for a good fit where normalized residuals are large. Conversely, it will tolerate bad fits where normalized residuals are small. I think we have seen some curve skewing in the present rerun of the sintered screen sample.

Correlations

We now get to the matter of comparing present parameter estimates for data set nh09-18 to those reported previously for data set nh05-07.

Overall Heat Flux

The most straight-forward comparison is in terms of overall heat flux N_q. The present results are skewed somewhat compared to before. We seem to have about 25% more heat flux at $P_{em} \approx 1$, about the same at $P_{em} \approx 100$ and about 10% less at $P_{em} \approx 1000$. Possible reasons for low-end discrepancy may be improved static conduction estimates, corrected thermistor noise or improved accuracy due to more and better-distributed data points. High-end discrepancy is more difficult to account for but may simply be due to many more data points logged at $P_{em} > 500$ — about 53 compared to 11. Actual correlating parameters and 90% confidence intervals are:

	present	previous
a_1	0.513 ± 0.030	0.396 ± 0.022
a_2	1.260 ± 0.098	1.316 ± 0.009

The confidence intervals quoted for the *previous* case are probably too high by a factor of about two because the residuals for the nh05-07 data set were high by about that same factor. Therefore, the present confidence intervals are actually about two times better than before, principally because we logged about four times as many data points.

Although I do not show residual plots for N_q modeling, the results suggest that our correlating expression is *not* a particularly good fit to the data — at least over the R_{em} range in question. The overall measure of curve-fit-to-data is the minimum achieved χ^2 value (sum of squared normalized residuals), which was 363 for N_q modeling. The theoretical most likely χ^2 minimum for normally distributed residuals is 192 (194 - 2) for 194 data points and 2 estimated parameters. A value of 363 is *extremely* unlikely (probability $< 10^{-12}$ — given a good fit to the data).

N_{ue} and (N_u, N_k)

We have a similar skewing of results for effective Nusselt number N_{ue} and simultaneous Nusselt number, enhanced axial conductivity ratio (N_u, N_k) estimates. Interesting is that now the simultaneous (N_u, N_k) reduction produces significantly better χ^2 estimates (minimum $\chi^2 = 213$) than N_{ue} estimates (minimum $\chi^2 = 363$). This is to be expected because of using three rather than two modeling parameters, but gives some corroboration to the reality of N_k. Previously, for some reason, this was not so dramatic. Actual correlating parameters for N_{ue} are:

	present	previous
a_1	0.288 ± 0.016	0.368 ± 0.020
a_2	0.740 ± 0.010	0.684 ± 0.009

and for (N_u, N_k) are:

	present	previous
a_1	0.844 ± 0.100	0.572 ± 0.094
a_2	0.572 ± 0.020	0.618 ± 0.025
a_3	3.561 ± 0.48	1.699 ± 0.69

Again, present confidence intervals are to be believed while previous ones were about half as large as they should have been.

Conclusions

The most important lesson to be drawn from this test-sample rerun is that we must make certain our normalized residual plots are reasonable before we can have confidence in estimated parameters and their confidence intervals. For the present data in particular, they are reasonable and I do have confidence in the estimated parameters.

Our increased number of data points logged and their weighting toward the low and high R_{em} extremes are now suggesting that the current correlating expressions for overall heat flux N_q and effective Nusselt number N_{ue} are not very good fits to the data. When our measurement error improves (as it surely will over the course of time) we can expect the misfit to become even more glaring. We shall probably have to spend some time dreaming up improved correlating expressions for N_q and N_{ue} — either with different functional forms, more parameters or, perhaps, piecewise defined over limited ranges of Reynolds number.

Still promising is simultaneous N_u and N_k data reduction. At our present limits of resolution, we seem to be able to fit the data pretty well although the residuals of figure 1 are beginning to show some systematic deviations at the extremes of R_{em}. Perhaps our present success is simply due to having three parameters to play with rather than only two. The test for this will come when we compare results for different test samples. If N_u and N_k values so obtained show some regular pattern from sample to sample then we will have further assurance that we are correlating real physics. If, on the other hand, N_u and N_k values diverge wildly we will conclude that we are fooling ourselves and be forced to dream up new correlating expressions to be put to the test.

APPENDIX B: RESULTS OF 1/2 LENGTH 1/2 MIL BRUNSWICK TESTS

Memo

To: Gary Wood
From: David Gedeon
Subject: Regenerator Test Rig: 1/2 mil Brunswick Rerun
Date: October 20, 1992

A rerun of the 1/2 mil Brunswick sample at half its former length, with reduced rig thermal noise and more data points logged, produces more accurate parameter estimates.

Background

Previous testing of the 1/2 mil Brunswick sample suffered from poor resolution at low R_{em} because measured heat flux was comparable to thermal noise level. We decided to improve matters by re-testing the same material at half its former length. Halving sample length roughly doubles axial temperature gradient and thereby doubles heat flux for a given R_{em}.

Meanwhile, we have also taken steps to reduce thermal noise. New with these tests is an Omega-brand low-pressure-drop coolant flow meter used in conjunction with a constant-head gravity feed water supply. The previous water supply was a direct connection to city water pressure and its attendant toilet-flush variations. Noise introduced by coolant flow variations is now noticeably reduced.

Another purpose of these tests is to check for errors in our data reduction process or test-rig physical assumptions. Our models presume overall heat flux varies linearly with sample temperature gradient, allowing us to normalize our correlating expressions to be independent of temperature gradient. Re-estimating parameters with a doubled temperature gradient should check-out both our theory and measurements.

Previous full-length tests were in file nh05-21. Present tests are in data files 2-10-(07B, 08C, 09B, 09E, 12E, 12G, 12H), ultimately combined into master file nh10-07.drv. The combined file contains 271 data points compared to about 90 before. R_{em} ranges from 0.79 to 540 in nh10-07 compared to 2.6 to 470 in nh05-21.

New Error Estimate

I have also revised the error estimate for neglected model term $\{c_p g T_s\}$ as part of the "relative error induced by neglected terms" plot printed after data modeling. This error is discussed on page 72 of the SBIR Phase I final report. Preliminary modeling runs produced unacceptably large values for said error (relative error about 1.6 at $R_{em} \approx 500$). So, I actually calculated a worst-case value from GLIMPS output (based on first-harmonics for g and T_s) and discovered it was about 1/10 as big as estimated. On this basis I have introduced

a correction factor of 1/10 into my previous error estimate. The question is, does this correction factor apply across the board or does it vary as a function of some unknown quantity? The answer is, I don't know. Estimating $\{c_p g T_s\}$ from first principles is to complicated for my small brain. (The main difficulty is estimating the phase angle between g and T_s.) Thus I find myself recommending that we apply the 1/10 correction factor across the board, with the standard remark that it is good enough for an error estimate.

New Modeling Program Naming Conventions

Starting with this data, I have changed the naming conventions for the various data modeling implementations. The following prefixes now apply:

prefix	purpose
RRP	f modeling
RRQ	overall N_q modeling
RRHE	effective N_{ue} modeling
RRHK	simultaneous (N_u, N_k) modeling

Program name are further indexed by numerical digits (RRHK1, RRHK2, etc.) for variations in correlating expressions.

Residuals

Our ever-improving thermal noise level and our tendency to log more-and-more data points are shedding new light on our models. Residual plots that used to be visually identical regardless of how we were modeling the data, now show significant model-related differences. For example, our two-parameter models for overall heat flux N_q and effective Nusselt number N_{ue} now show significant systematic deviations from the data while our three-parameter model for simultaneous (N_u, N_k) seems to fit within the limits of our resolution over the entire range of R_{em} tested. This is evident in figure 1 which shows various residual plots for the present data set. Incidentally, the appearance of the (N_u, N_k) residuals and their minimum χ^2 value suggest our present error estimates are reasonable.

Correlations

The following tables compare present parameter estimates for data set nh10-07 to those reported previously for data set nh05-21. I have corrected confidence intervals for the nh05-21 data by multiplying by a factor of 1/2 to account for the input error estimates being about 2 times bigger than they should have been.

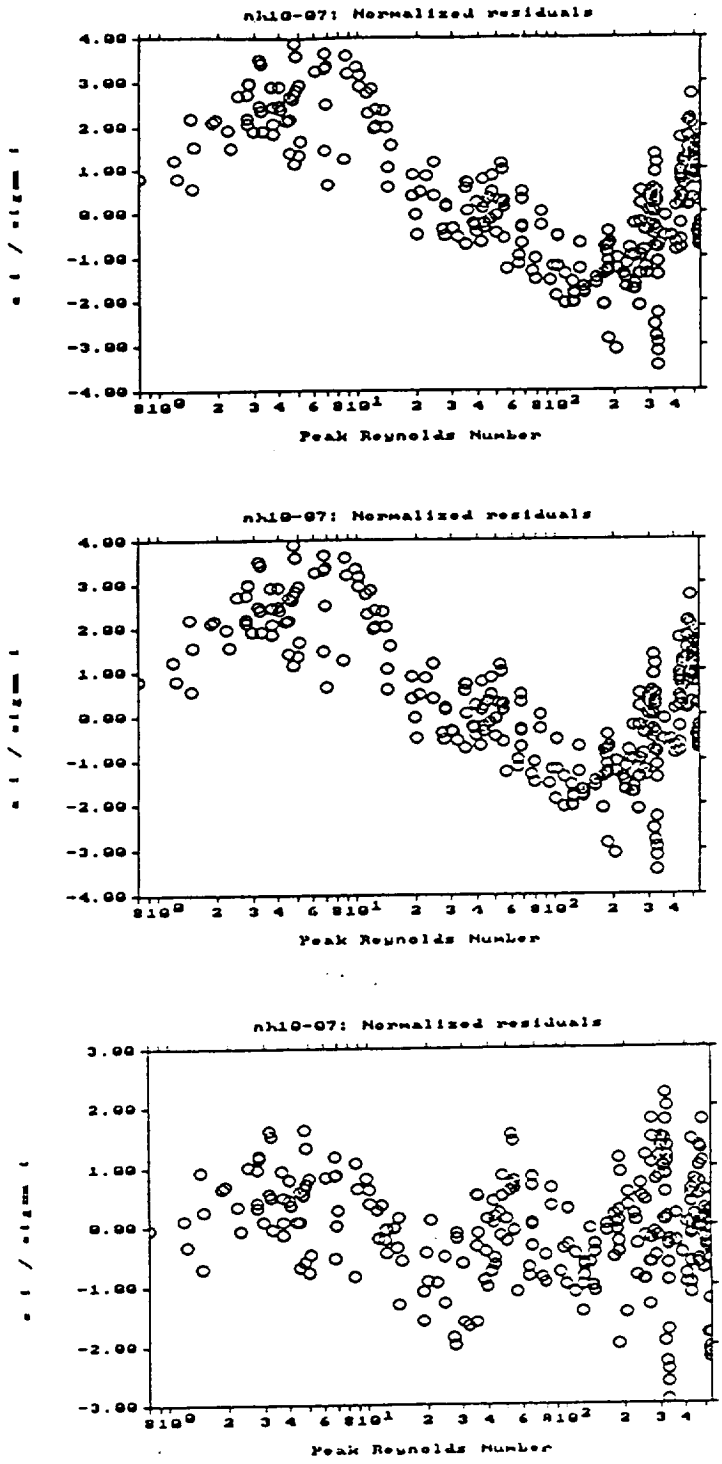

Figure 1: Residuals in the present data set for overall heat flux N_q modeling (top, $\chi^2 = 684$), effective N_{u_e} modeling (middle, $\chi^2 = 683$) and simultaneous N_u and N_k modeling (bottom, $\chi^2 = 271$)

Overall Heat Flux

Overall heat flux parameters agree well between the present and former data sets, even though the N_q model equation does not fit the data particularly well. Actual correlating parameters and 90% confidence intervals are:

	present	previous
a_1	0.480 ± 0.015	0.425 ± 0.024
a_2	1.223 ± 0.006	1.232 ± 0.011

Evaluated at some representative R_{em} values we get

R_{em}	N_q present	N_q previous
1	0.480	0.425
10	8.02	7.25
100	134	124
500	959	898

We may attribute disagreement at low R_{em} to improved resolution of the present tests. I see no clear reason for the disagreement at high R_{em}, although it amounts to only about 7% at $R_{em} = 500$. This discrepancy is roughly consistent with the quoted confidence intervals so I'm not going to worry about it. I conclude that halving the test-sample length does not significantly affect the estimated parameters.

Effective N_{ue}

Again, estimated parameters agree well between present and former data sets. Actual correlating parameters for N_{ue} are:

	present	previous
a_1	0.311 ± 0.009	0.350 ± 0.019
a_2	0.777 ± 0.006	0.767 ± 0.011 .

Evaluated at some representative R_{em} values we get

R_{em}	N_{ue} present	N_{ue} previous
1	0.311	0.350
10	1.86	2.05
100	11.1	12.0
500	38.9	41.1

Conclusions similar to those above for N_q apply here too.

Not one to leave well enough alone, I couldn't resist trying to improve upon the fit-to-data of our correlating expression for N_{ue}. Recall that our present two-parameter correlation is

$$N_{ue} = a_1 P_e^{a_2} \tag{1}$$

I first evaluated a three-parameter form as follows:

$$N_{ue} = a_1 + a_2 P_e^{a_3} \tag{2}$$

Unfortunately a_1 kept going negative during the parameter estimating processing, causing numerical trouble. I then fell back to an alternate two-parameter form based on a Reynold's analogy applied to the Ergun-form friction factor:

$$N_{ue} = a_1 + a_2 P_e \tag{3}$$

This converged OK but showed even worse fit to the data than the original two-parameter form. I am temporarily stymied.

Simultaneous (N_u, N_k)

This time parameters have changed dramatically between present and former data sets. This is explained by a shift in the perceived relative importance of enthalpy flux compared to enhanced axial conduction. I suspect that the increased number of data points at the low R_{em} extreme, and lower noise there, have a lot to do with the shift. Actual correlating parameters for (N_u, N_k) are:

	present	previous
a_1	0.991 ± 0.065	0.498 ± 0.124
a_2	0.582 ± 0.012	0.711 ± 0.041
a_3	2.496 ± 0.18	0.600 ± 0.43

Evaluated at some representative R_{em} values we get

R_{em}	N_u present	N_u previous	N_k present	N_k previous
1	0.911	0.498	2.50	0.600
10	3.48	2.56	9.53	3.08
100	13.3	13.2	36.4	15.8
500	33.9	41.3	92.9	49.7

We seem to have here a variation of the Heisenberg uncertainty principle applied to data modeling. Namely: The more parameters we use, the more accurate the fit to data but the less accurate the parameters themselves are estimated.

Even so, I was tempted to again resurrect the original four-parameter form:

$$N_u = a_1 P_e^{a_2} \tag{4}$$

$$N_k = a_3 P_e^{a_4} \tag{5}$$

this is compared to the baseline three parameter form with common exponent:

$$N_u = a_1 P_e^{a_2} \tag{6}$$

$$N_k = a_3 P_e^{a_2} \tag{7}$$

I am half-way enthusiastic about the result which was

$$
\begin{array}{ll}
a_1 & 0.612 \pm 0.089 \\
a_2 & 0.658 \pm 0.024 \\
a_3 & 2.998 \pm 0.26 \\
a_4 & 0.342 \pm 0.090
\end{array}
$$

The fit to data was slightly better than the three-parameter form (minimum $\chi^2 = 205$ compared to 227), but confidence intervals for the exponents are much worse (especially for a_4). Perhaps we will do better in the future as our rig evolves?

My reason for trying the four-parameter form was that it promises to strengthen our case for simultaneous N_u and N_k modeling. Recall that the validity of our three-parameter estimates requires the following two assumptions:

1. That exponential expressions are valid for N_u and N_k
2. That the exponents for both are equal

Four-parameter estimation eliminates the need for the second assumption. We need only believe that exponential forms are valid. Perhaps this is within the realm of theory to prove?

Conclusions

A notable conclusion is that our rig and data reduction software have once again passed the reputability test. That is, they produced nearly the same correlations for N_q and N_{ue}, even when sample length was halved. Thank God.

On the never-a-dull-moment front, we continue to see new research opportunities open up before us. Somebody needs to dream up improved correlating expressions for N_q and N_{ue}. I am open to suggestions here. Regarding simultaneous (N_u, N_k) modeling, we seem to be at a critical juncture. On the one hand, the presently-fashionable three-parameter form converges nicely and fits the data well but requires the ad-hoc assumption that the exponents (in the expressions for N_u and N_k) are equal. The four-parameter form, on the other hand, converges less reliably and with sloppier confidence intervals but does not require equal exponents. In fact, it seems to be telling us that the exponents are *not* equal. So which form do we use? The interests of expediency might suggest the three-parameter form is good enough. But the quest for absolute truth seems to demand we try harder with the four-parameter form. Helpful in this regard would be even lower thermal noise. Stay tuned.

APPENDIX C: RESULTS OF 80 MESH SCREEN PRESSURE DROP TESTS

Memo

To: Gary Wood
From: David Gedeon
Subject: Regenerator Test Rig: 80-Mesh Screen Pressure-Drop Tests
Date: October 30, 1992

In which we return to pressure-drop testing and the state of the art evolves noticeably.

Background

Reported here are pressure-drop test results for 80 mesh (per inch) stainless-steel screens, porosity = 0.7102, wire diameter = 93.98 microns (.0037 in), sample length = 22.08 mm.

Data files are 2-10-(13A, ..., 13C, 16A, ..., 16E), combined into overall file nh-10-13. During preliminary data modeling, a close examination of residuals showed that input error estimates Pfast_err and X_err could use some work. This is the topic of the next section of this memo. Following that digression I'll get down to results.

Calculating Input Error Estimates From Residuals

Normalized Residuals are supposed to be randomly distributed about zero with unit variance, uniformly across the range of peak Reynolds numbers — at least when the model fits the data. Remember, a normalized residual for the i-th data point may be written symbolically

$$\text{Normalized Residual} = \frac{y_i - y(x_i)}{\sigma_i} \tag{1}$$

where $y_i - y(x_i)$ is the difference between the measured and theoretical experimental variable and σ_i is an estimate of random measurement error. Observed residual variance greater or less than than unity means that the σ_i error estimates are incorrect. I saw this in our data. Initial data modeling showed normalized residuals with variance much less than unity at low R_{em} and somewhat greater than unity at high R_{em}. Error estimates thus indicted, we ask what went wrong and how to fix it.

Recall that the σ_i for pressure drop testing are the estimated errors in test-sample pumping dissipation. The actual error estimating formula is outlined on p. 62 of the SBIR phase I final report. For purposes here it is sufficient to mention that the estimated dissipation error is the root-sum-squared of two terms. Term 1, say σ_p, is proportional to fast-pressure transducer error Pfast_err and term 2, say σ_x, which is proportional to position transducer error X_err. In math notation,

$$\sigma^2 = \sigma_p^2 + \sigma_x^2 \tag{2}$$

Both Pfast_err and X_err are inputs. What went wrong then is that Pfast_err and X_err were initially set incorrectly — their values did not reflect the true random-sampling error in their respective signals. How to fix it, is to use the residuals themselves to back-out more reasonable values for Pfast_err and X_err.

I must point out that correctly setting Pfast_err and X_err is a non-trivial task. We are asking here for the standard deviations of fast-pressure and position signals in the sense of random-sampling error, rather than systematic error, and after filtering through the Fourier-analysis routines of the data acquisition program, rather than for the raw transducer outputs. It is not surprising that we might not to know the correct values in advance.

The basic idea for evaluating Pfast_err and X_err is this: We first make trial inputs for both, run the data modeling program and take note of the resulting minimum chi-squared value χ^2_m. Remember the χ^2 function is just

$$\chi^2 = \sum_{i=1}^{N} \left(\frac{y_i - y(x_i)}{\sigma_i} \right)^2 \tag{3}$$

Then we can compare said χ^2_m to the theoretical value for correctly estimated σ's, say χ^2_t, which we know tends to $N - M$, where N is the number of samples and M is the number of parameters estimated. If $\chi^2_m \gg \chi^2_t$ we suspect our error estimates are too small, and vice-versa. In fact, from the above equation, we conclude that our input σ's compare to the correct values, on the average, according to the equation

$$\sigma^2/\sigma_t^2 = \chi^2_t/\chi^2_m \tag{4}$$

where σ_t stands for the correct error estimates. On this basis we can fiddle with Pfast_err and X_err to make $\sigma^2 = \sigma_t$.

An astute reader might object that it would not be possible to uniquely solve for Pfast_err and X_err by this means because there are infinitely many combinations that would produce the same combined error σ. True enough, but a key observation is that the relative importance of error terms σ_p and σ_x varies with peak Reynolds number. Therefore, if we split our data set into a low-R_{em} part and a high-R_{em} part we should be able to succeed.

Here are the details as they apply to our specific problem: High- and low-R_{em} values are in data sets 2-10-13A and 2-10-16E, containing 48 and 66 data points, respectively. I ran the data modeling program on each of these with the following orthogonal basis of trial values:

	Pfast_err (Pa)	X_err (m)
Case 1	10	0
Case 1	0	5.0E-5

The reason I call these cases *orthogonal* is that the combined error σ^2 is just $\sigma^2 = \sigma_p^2$ for case 1 and $\sigma^2 = \sigma_x^2$ for case 2. Using equation (4), I was able to

determine that for the low-R_{em} part of the data

$$\sigma_p^2/\sigma_t^2 = 3.31 \quad (5)$$

$$\sigma_x^2/\sigma_t^2 = 1.38 \quad (6)$$

and for the high-R_{em} part of the data

$$\sigma_p^2/\sigma_t^2 \approx 0 \quad (7)$$

$$\sigma_x^2/\sigma_t^2 = 1.84 \quad (8)$$

Next I defined two scale factors, a and b, by the requirement that $a\sigma_p^2 + b\sigma_x^2 = \sigma_t^2$ in both data sub-sets. The idea is that by scaling the trial values of Pfast_err and X_err by $\sqrt{a}$ and $\sqrt{b}$, respectively, we will wind up with $\sigma^2 = \sigma_t^2$, which is what we want. Evidently we must solve the linear system

$$3.31a + 1.38b = 1 \quad (9)$$

$$0a + 1.84b = 1 \quad (10)$$

No problem. The solution is $a = 0.077$ and $b = 0.54$, and the best-guess values for our error inputs are, therefore:

$$\text{Pfast\_err} = 10\sqrt{0.077} = 2.8 \quad (11)$$

$$\text{X\_err} = 5 \times 10^{-5}\sqrt{0.54} = 3.6 \times 10^{-5} \quad (12)$$

The reason I have bothered being so specific about details is that we may have to do this again sometime. In fact, re-setting, or at least checking, input error estimates like this should be standard practice. Correctly estimating errors insures two things:

- That our parameter estimates are given equal weight over the entire R_{em} range
- That we have an accurate independent basis for determining fit to data.

The first statement is true because the basis for parameter estimation is the χ^2 value. If normalized residuals are weighted low over some range of R_{em}, then the software will tolerate a sloppier fit there. Or vice-versa. The second statement is true because, given good error estimates, a minimum χ^2 value that is significantly too large can mean only one thing: the correlation does not fit the data. I should mention that this is not necessarily bad. It is inevitable as instrumentation improves more and more. Eventually we will always get to the point where we cannot fit the curve to the limits of our precision. But, the fit we do get may be good enough for most engineering purposes.

Results

This data set has led me to conclude that the previous two-parameter form for friction factor

$$f = a_1/Re + a_2 \tag{13}$$

is no longer acceptable. To see the basis for my conclusion turn to the residual plot at the top of figure 1. Note the systematic deviations from zero completely overwhelm any randomness. The minimum χ^2 value for these residuals is about 3.65E4 compared to the expected minimum of 276 for a good fit to data.

The problem is more pronounced now than for previous data modeling for two reasons. First, we have more reasonably set our error inputs Pfast_err and X_err according to the above process, thereby making systematic deviations from the theoretical curve more apparent — especially at low R_{em}. Second, the maximum R_{em} is about 6000, much higher than ever before. At high Reynolds numbers classic references such as Kays and London [1] clearly show that the curve of screen friction factor vs Reynolds number retains a negative slope, contrary to the constant asymptotic value of $f = a_2$ implied by the two-parameter Ergun equation. Our data seems to agree with Kays and London.

I was able to get a much better fit to data by introducing a relatively minor modification to the Ergun form. I call this the three-parameter modified Ergun form:

$$f = a_1/Re + a_2 R_e^{a_3} \tag{14}$$

The idea is that parameter a_3 will be negative but small, allowing the correlation to better track reality at high R_e. Residuals for the modified Ergun form are shown at the bottom of figure 1. The minimum χ^2 is now 1.29E3, much better than before but nowhere near the expected value of 275. Evidently there remains some non-random component to the residuals for the modified Ergun equation, although it no longer completely overwhelms the random component. As mentioned before, some systematic deviation between theory and experiment is inevitable. With our present error inputs of Pfast_err = 2.8 Pa (!!) and X_err = 36 microns, I feel we can tolerate the present degree of slop and still be quite good enough for most engineering applications.

The final estimated parameters and 90% confidence intervals for the modified Ergun form are

a_1	118.7 ± 0.3
a_2	2.655 ± 0.016
a_3	-0.09734 ± 0.00080

References

[1] W.M. Kays, A.L. London, *Compact Heat Exchangers, 3rd Edition*, McGraw-Hill, (1984)

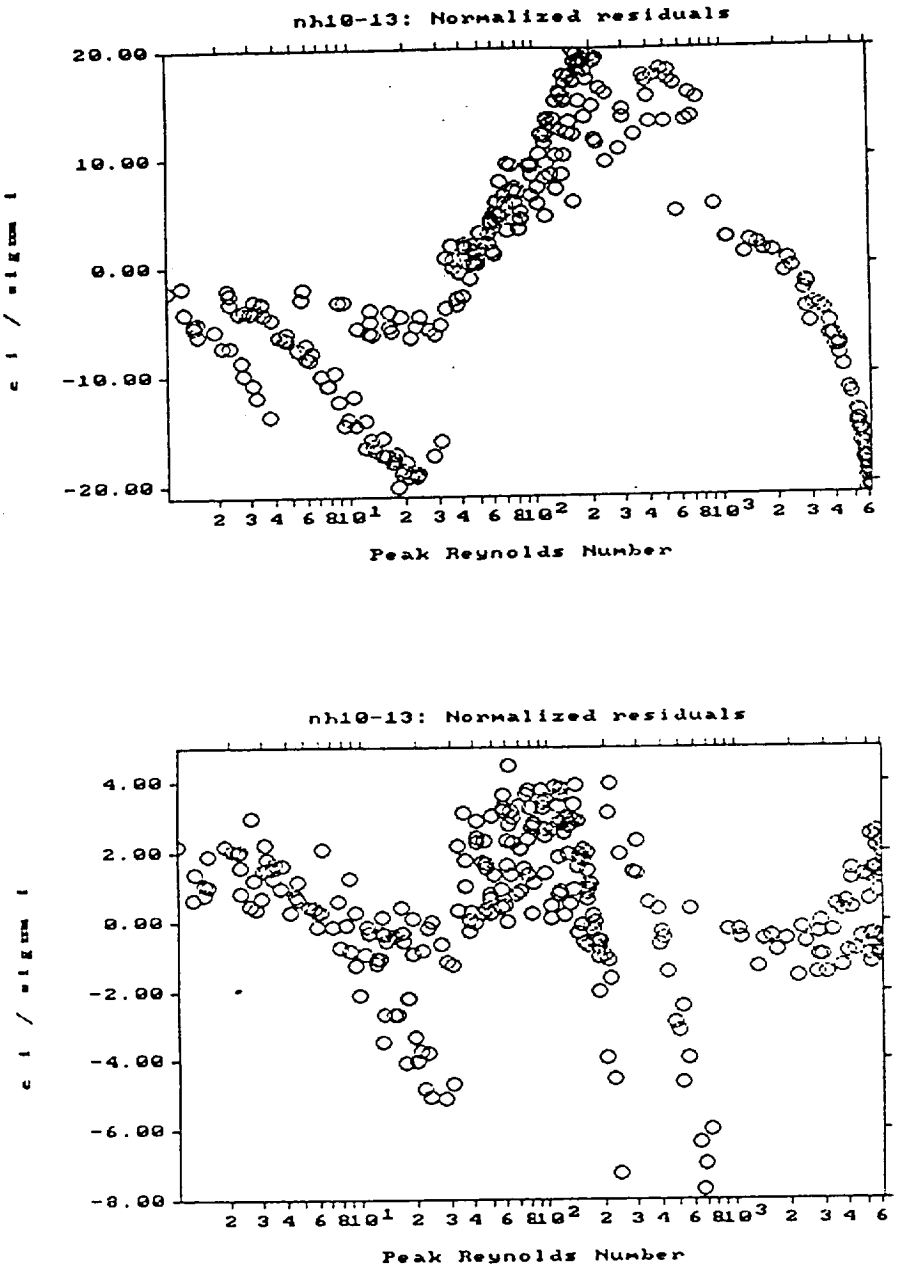

Figure 1: Normalized residuals for previous two-parameter Ergun-form friction factor (top) and modified three-parameter form (bottom). (Note the difference in scales)

APPENDIX D: DATA (Contained on three diskettes supplied to the NASA-Lewis Technical Monitor)

2.0 mil Brunswick:

Heat Transfer	2-11-21	B...E	(omit pts D 1; E 1-4)
	2-11-22	A,B,D,E	(omit B 1-9)
Pressure Drop	3-6-29	A...D	

1.5 mil Brunswick (top piece)

Heat Transfer	2-11-23	B...I	(omit pts B 1-4; G 1-3; H 1)
Pressure Drop	3-6-30	A...D	

1.5 mil Brunswick (middle piece)

Heat Transfer	3-3-10	D...F	(omit pts D 1-9)
	3-3-11	A...D	(omit pts D 1,3,15)
Pressure Drop	3-6-2	A...F	(diffuser length should be 0)

1.0 mil Brunswick

Heat Transfer	2-11-18	G...I	
	2-11-19	A...F	(omit B1-3,29; D25; E3)
Pressure Drop	2-11-4	A...D	(C should be He)

0.5 mil Brunswick (1/2 length)

Pressure Drop	2-11-3	F...J	

200 mesh Sintered Screen

Heat Transfer	2-11-17	H...J	(omit H1-34; I1,29,31)
	2-11-18	B...F	(omit B1-6; C45&46; D31; E1,2,29,30,41; F1)
Pressure Drop	2-11-3	A...E	

100 mesh Stacked Screen

Heat Transfer	2-11-16	B,D...F	
	2-11-17	B,D,G	(omit D34)
Pressure Drop	2-11-4	E.....H	

80 mesh Stacked Screen

Heat Transfer	2-11-12	B,D..I,K
Pressure Drop	2-11-2	A....G